Chain Mobility in Polymer Systems: On the Borderline between Solid and Melt. 3. Phase Transformations in Nascent Ultrahigh Molecular Weight Polyethylene Reactor Powder at Elevated Pressure As Revealed by in Situ Raman Spectroscopy

L. Kurelec,[†] S. Rastogi,*[,†] R. J. Meier,[‡] and P. J. Lemstra[†]

Eindhoven Polymer Laboratories/The Dutch Polymer Institute, Eindhoven University of Technology, P.O. Box 513, 5600 MB Eindhoven, The Netherlands; and DSM Research, P.O. Box 18, 6160 MD Geleen, The Netherlands

Received July 12, 1999; Revised Manuscript Received November 24, 1999

ABSTRACT: The phase transformations under elevated pressure have been followed in situ by X-ray and Raman spectroscopy for ultrahigh-molecular-weight polyethylene (UHMW−PE) reactor powder. Using the in situ X-ray as a reference for the Raman work, it has been shown that Raman spectroscopy is a convenient method to follow phase transformations in polyethylene under pressure. The distinction has been made between different solid phases in polyethylene (monoclinic, orthorhombic, and hexagonal phases) and the melt by studying the conformational changes occurring within the skeletal mode (1000−1200 cm^{-1}) upon the phase transformations. The crystal field splitting (1415/1440 cm^{-1}) in the $-CH_2-$ bending mode of the Raman spectrum of polyethylene, related to the orthorhombic unit cell, was confirmed to be sensitive to transformations between different crystal structures. By following the changes occurring in the methylene bending mode together with the changes within the C−C skeletal mode, it has been shown that the crystalline phases and the melt can be mutually distinguished.

1. Introduction

Linear polyethylene can be considered a model system in the study of nucleation and growth[1] as well as in the understanding of the fundamentals concerning phase transformations in polymer systems.[2] At ambient conditions (pressure and temperature) it crystallizes in the orthorhombic unit cell with the molecular chains in a trans-zigzag conformation. The thickness of the crystals is much less than the fully extended length of the polymer chain because the chains within the crystal fold back and forth forming well-established folded chain crystals (fcc).[3] A different type of morphology can be obtained when crystallizing PE under elevated pressures (above 3.6 kbar) and temperatures. Instead of relatively small folded chain crystals, polyethylene crystallizes into large entities possessing a thickness up to a few micrometers. The morphological difference between the two types of crystals obtained under different crystallization conditions is due to the appearance of an intermediate phase,[4] thermodynamically stable above 3.6 kbar and 200 °C. In this phase, chains are sufficiently mobile to allow the crystal to grow simultaneously in the lateral and thickness direction leading to the formation of extended chain crystals (ECC).[5−8] The crystal structure of the intermediate phase was determined to be hexagonal.[9] It has been shown recently using time-resolved X-ray, available at the Synchrotron Radiation Facilities in Grenoble, France, that the stability of the hexagonal phase can be obtained at much lower values of pressure and temperature than reported earlier,[10,11] depending on the initial morphology, notably the crystal size. The enhanced chain mobility in the hexagonal phase, as well as its appearance at sufficiently low pressures and temperatures, is suggested to be a route to process the usually intractable UHMW−PE powder resulting in products possessing improved properties.[12] Those developments stimulated the research for methods that allow us to monitor in situ phase transformations in polyethylene at elevated pressures.

Many studies, using different experimental techniques (high-pressure DTA,[4,13,14] dilatometry,[15,16] wide-angle X-ray spectroscopy,[9,17,18] NMR[19,20]) have been performed on polyethylene at elevated pressure. The main purpose of these studies was to resolve the exact molecular structure of the hexagonal phase. Detailed studies on the crystallographic parameters of the hexagonal and orthorhombic phase suggested that the polyethylene molecules in the hexagonal phase possess mainly gauche conformation.[18] The molecular packing of the phase has therefore been defined as "a liquid-crystalline" one.

Raman spectroscopy has been also used as a technique to follow changes in the chain conformation of polyethylene in the hexagonal phase. Since no distinction between the Raman spectra of the hexagonal phase and the melt could be observed by Takamura[19,21] et al. and Wunder,[22] the authors concluded that a conformational disorder similar to the melt exits in the intermediate hexagonal phase. Recently, Tashiro[23] et al. tried to show the usefulness of the Raman spectroscopy in the identification of the orthorhombic to hexagonal and the hexagonal to melt transitions. To avoid complicated setups, needed to enter the high-pressure region of the hexagonal phase, the experiments were performed on constrained ultrahigh modulus fibers, which before melting, pass through the hexagonal phase.[24,25] The results were discussed in the combination with IR and X-ray data. A clear distinction between the orthorhombic to hexagonal and the hexagonal to melt transition

* To whom correspondence should be addressed.
[†] Eindhoven University of Technology.
[‡] DSM Research.

10.1021/ma9911187 CCC: $19.00
Published on Web 06/27/2000

was shown by in situ X-ray scattering and IR spectroscopy, whereas no distinction between the hexagonal phase and the melt could be made by Raman spectroscopy. The insensitivity of the Raman spectroscopy to distinguish between the hexagonal phase and the melt was related to trans sequential length being shorter than five CH_2 units in the hexagonal phase.[26]

So far no experimental observations have been reported which follow in real time the appearance of the hexagonal phase under pressure making use of X-ray and Raman spectroscopy under same conditions. In this paper, the first in situ experimental observations by X-ray and Raman spectroscopy on polyethylene under pressure will be presented. Unlike the previously reported observations it will be shown that the distinction between the orthorhombic and the hexagonal phase as well as the melt can be obtained using Raman spectroscopy. Next to the three phases mentioned so far (orthorhombic, hexagonal, melt) the onset of the monoclinic phase in polyethylene under increased pressure at room temperature will also be reported. The transition from the orthorhombic to the monoclinic phase is followed by in situ X-ray and Raman spectroscopy. The origin of this transition is explained as a result of shear.[27−30]

2. Experimental Section

2.1. Materials. For this study the same nascent UHMW−PE powder as the one used for our previous studies is used.[12] The reactor powder possessing a M_w of 3.5×10^6 g/mol was kindly synthesized for our purposes by DSM. A relatively small crystal size (estimated fold length 8−10 nm) is characteristic for this powder grade polymerized at low temperatures.

2.2. Instrumentation. In this study we made use of a pressure cell similar to the one designed by Hikosaka and Seto.[31] The maximum attainable pressure in the current setup is 5 kbar, and the temperature can be varied from room temperature up to 300 °C. The sample of 0.4 mm thickness is placed between two diamond windows, each having a thickness of 1 mm. Use of diamond windows enables in situ observation by polarizing microscopy as well X-ray diffraction and Raman spectroscopy. The sample, sandwiched between two diamond windows, is surrounded by Teflon spacer rings. Pressure on the sample is generated hydrostatically with the help of two pistons activated by regulated nitrogen gas. Because of the smooth motion of the pistons, the pressure is kept constant throughout the experiments.

In situ X-ray experiments were performed using monochromatic X-rays of wavelength 0.798 Å and a high flux available on beamline ID11-BL2, at the European Synchrotron Facilities in Grenoble, France. The lower wavelength was required to avoid the X-ray absorption from the diamond windows. Each diffraction pattern was recorded for 15 s on a two-dimensional CCD detector. Using the FIT2D program of Dr. Hammersly (ESRF), 2D X-ray patterns were transformed into one-dimensional patterns by performing an integration along the azimuthal angle.

Raman spectroscopy was recorded with a Labram spectrometer from Dilor S. A. (France). A Spectra Physics Millenium II Nd:YVO_4 laser at 532 nm was used as an excitation source. The initial laser power was 0.20 W. Laser light was focused on the sample using a slit width of 100 μm and a 20× microscope objective. The backscattered light from the sample was dispersed with an 1800 mm^{-1} grating on the CCD detector. The analysis of the Raman spectra involved baseline correction and curve-fitting procedure. The curve fitting has been performed in two ways: (i) using the GRAMS package including Voigt line profiles[32] and (ii) LabSpec software using Gauss line shape. All Raman spectra are displayed along the *y*-axis for reasons of clarity, but no rescaling has been applied to any spectrum.

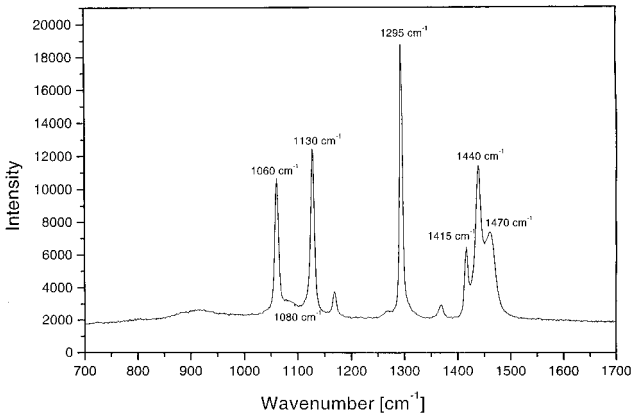

Figure 1. Raman spectrum of the nascent UHMW−PE powder under ambient conditions. The Raman bands denoted in the figure are assigned to the following vibrational bands:[39,44] 1060 cm^{-1}, asymmetric C−C stretching vibration in crystalline domain; 1080 cm^{-1}, C−C stretching in amorphous polyethylene; 1130 cm^{-1}, symmetric C−C stretching, crystalline; 1295 cm^{-1}, CH_2 twisting, crystalline; 1415/1440 cm^{-1}, crystal field splitting of the bending vibrational mode.

3. Scientific Background: Raman Spectroscopy of Polyethylene

Before proceeding with the experimental observations, a brief summary of the salient findings on the conformational Raman bands of polyethylene reported in the literature will be given in this paragraph.

The phase transformations of polyethylene at elevated pressure and temperature will be discussed in the spectral region between 700 and 1700 cm^{-1}, which can be divided into three different regions.[33] The first region, see Figure 1, is the skeletal C−C vibration mode between 1000 and 1200 cm^{-1}. It consists of two narrow bands representing respectively in-phase and out-of-phase vibrations appearing at 1060 and 1130 cm^{-1} respectively. In the melt, a broad band centered around 1080 cm^{-1} becomes dominant while the bands at 1060 and 1130 cm^{-1} disappear completely. A relative measure of the trans-bond content has been given by the intensity ratio of either the 1060 or the 1130 cm^{-1} band to the intensity of the 1080 cm^{-1} band.[22]

The second region comprises the CH_2 twisting vibration mode, which can be distinguished at 1295 cm^{-1}. This region has been shown to be independent of conformational changes and is used as an internal intensity standard.[34,35] However, in our experimental setup the two diamond windows of the pressure cell give a strong phonon vibration around 1350 cm^{-1}. Upon heating, the phonon band from the diamond windows broadens and interferes with the CH_2 twisting mode of polyethylene. For this reason the mode is not used as an internal calibrant for the spectra recorded at the elevated temperatures (above 200 °C).

The third region of interest is the complex bending vibration mode between 1400 and 1500 cm^{-1}. It consists of the well-resolved triplet at 1415, 1440, and 1470 cm^{-1}. It has been well established that the bands at 1415 and 1440 cm^{-1} are the correlation split doublet corresponding to the $\delta(CH_2)$ mode of symmetry A_g for the single chain.[36] The experiments showed that the band at 1415 cm^{-1} originates from CH_2 in phase bending mode (A_g) and band at 1440 cm^{-1} from the CH_2 out of phase bending mode (B_{1g}).[37,38] The intensity ratio $I(A_g^+)/I(B_{1g}^-)$, is determined mostly by the setting angle between the two chains in the orthorhombic unit cell.[39]

The crystal field splitting is characteristic of the orthorhombic unit cell, occupied by two structural units (molecular chains).[40] The spectrum in the methylene bending range is, however, severely complicated due to the presence of combination bands and overtones, in particular the presence of Fermi resonance arising from the 720−731 cm^{-1} methylene rocking bands which are IR active. It has been shown that not only the two $k = 0$ CH_2 rocking modes may enter Fermi resonance, but also large sections of the $k \neq 0$ phonons in the two CH_2 rocking dispersion curves in the 700−740 cm^{-1} range also contribute to Fermi resonance in the bending region of the Raman spectrum of polyethylene.[39,41] From the Raman spectra of stretched-oriented polyethylene it has been shown experimentally[37] that the Raman line observed at 1470 cm^{-1} originates from B_{1g} overtones and binary combinations in Fermi resonance with the fundamental at 1440 cm^{-1}. The large set of overtones and combinations, in principle very weak, becomes noticeable only because this set shares intensity with the 1440 cm^{-1} fundamental. All of these contributions will strongly affect the quantitative analysis of this region of the spectra. Therefore, it has been suggested that the intensity ratio of the A_g/B_{1g} components of the factor-group split of CH_2 bending fundamentals has to be evaluated by considering the ratio between the 1415 cm^{-1} band and two other bands whose origin is taken to be B_{1g} ($I_{1415}/(I_{1440} + I_{1470})$).[39]

To define the phase transition in polyethylene under elevated pressure we will focus our discussion on the relative changes in the skeletal (1000−1200 cm^{-1}) and the bending (1400−1500 cm^{-1}) region. This method was also used in the interpretation of the Raman spectra of *n*-alkanes during heating at atmospheric pressure,[42,43] when *n*-alkanes undergo the first-order transition into the so-called rotator phase. It has been reported that the rotator phase is to some extent similar to the high-pressure hexagonal phase in polyethylene.[44] In the rotator phase, the typical C−C skeletal bands of Raman spectrum, characteristic of the trans-zigzag conformation, do not lose intensity, while the triplet in C−H bending region, characteristic of orthorhombic phase, merges into a broad singlet centered around 1440 cm^{-1}. These results lead to the conclusion that the chains in *n*-alkanes retain a relatively larger proportion of the all-trans conformation within the rotator phase compared to the hexagonal phase of polyethylene in constrained fibers.[23,42]

4. Results and Discussion

The discussion of the experimental results will be divided into two different sections. In the first part the orthorhombic to monoclinic phase transition (orth → mono) occurring on raising pressure at room temperature will be presented. In the second section the changes occurring on heating the sample at constant pressure of 4000 bar will be discussed in the terms of monoclinic to orthorhombic (mon → orth), orthorhombic to hexagonal (orth → hex) and hexagonal to melt (hex → melt) transitions. A schematic diagram of the routes used in this study is given in Figure 2. The phase transformations encountered on raising pressure and subsequent isobaric heating are followed by in situ X-ray and Raman spectroscopy.

4.1 Raising Pressure at Room Temperature. Figure 3 shows the X-ray patterns of the nascent UHMW−PE powder recorded in situ when raising pressure at room temperature. The starting diffraction pattern (Figure 3a), at 160 bar, is taken at the minimum attainable pressure within the pressure cell used in this study. Here, next to the usual (110) and (200) orthorhombic reflections a relatively strong (100) monoclinic reflection is also present, indicating that the part of the orthorhombic crystals transformed into the monoclinic ones. Because of the small initial crystal size, crystals are more likely to shear which results in the transformation from the orthorhombic to the monoclinic crystal structure at relatively low pressures.[45] To confirm the transformation, Figure 3g shows the X-ray diffraction pattern of the same UHMW−PE grade in its powder form at ambient conditions (out of the pressure cell). Here, the strong (110) and (200) orthorhombic reflections can be observed together with a relatively weak (100) reflection of the monoclinic phase. Nevertheless, on raising pressure the monoclinic (100) reflection intensifies while the (110) and (200) orthorhombic reflections loose intensity (Figure 3, parts a−f).

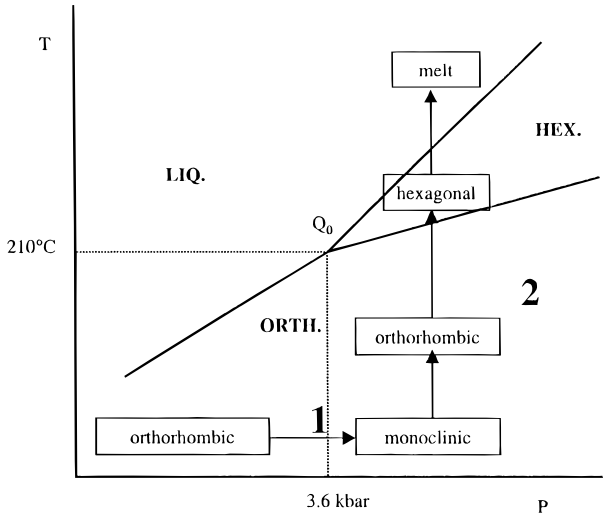

Figure 2. Schematic drawing of the experimental routes performed in this study. The route denoted with **1** is related to the phase transformations occurring while raising pressure up to 4000 bar at room temperature. The route denoted with **2** is related to the phase transformations occurring while heating the sample from 25 to 250 °C isobarically at 4000 bar.

The same set of time-resolved experiments was performed using Raman spectroscopy. The spectra in Figure 4 were recorded while raising pressure at room temperature under the same conditions as those of the WAXS experiments discussed above. In the starting spectra (at 160 bar) the anticipated triplet for the orthorhombic phase in the bending region (1400−1500 cm^{-1}) as well as the two narrow peaks corresponding to the in-phase and out-of-phase skeletal C−C vibrations (1000−1200 cm^{-1} spectral range) can be observed. From this spectrum alone the presence of the monoclinic phase cannot be clearly distinguished. Nevertheless, as the monoclinic phase strengthens with increasing pressure, changes in the vibrational bands in the region 1400−1500 cm^{-1} are observed. As stated earlier, the bending mode with its typical crystal field splitting is a measure of the orthorhombic crystal structure and the changes within this mode should be related to the changes concerning the phase transformation.

When raising the pressure, up to 4000 bar, as the monoclinic phase becomes dominant, the band at 1415 cm^{-1} loses intensity relative to the band at 1440 cm^{-1}, indicating the disappearance of the initially pronounced

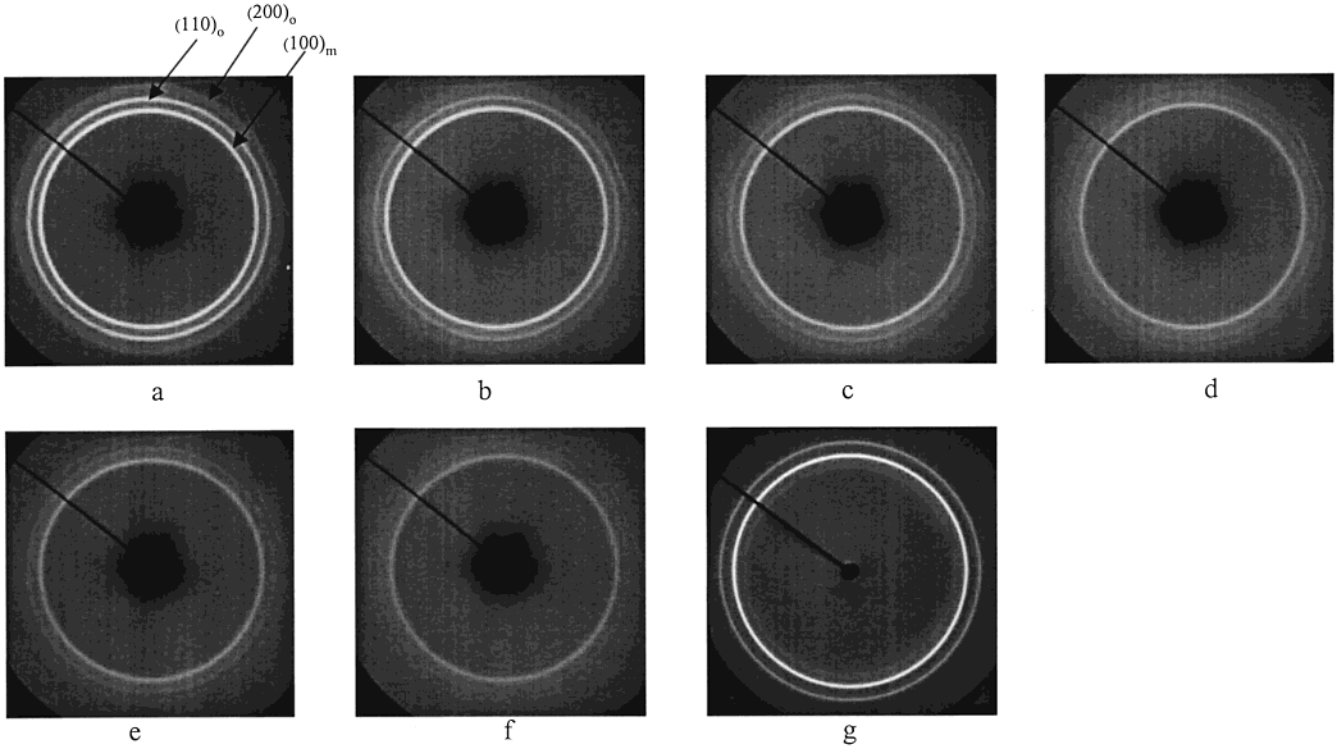

Figure 3. X-ray patterns of the nascent UHMW−PE recorded in situ when raising pressure at 25 °C: (a) 160 bar; (b) 960 bar; (c) 1760 bar; (d) 2400 bar; (e) 3400 bar; (f) 4000 bar; (g) ambient pressure (out of the pressure cell).

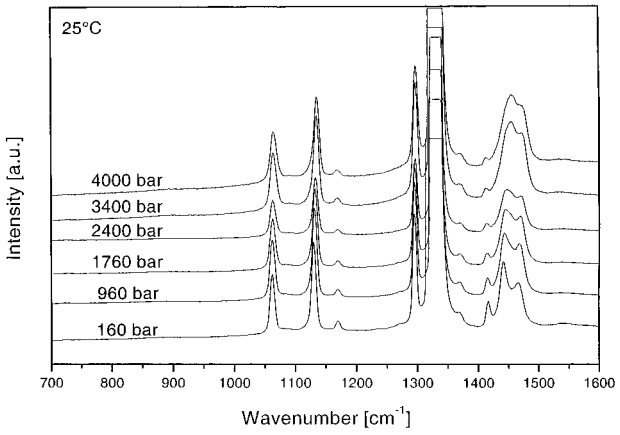

Figure 4. Raman spectra of UHMW−PE recorded in situ on raising pressure at room temperature, revealing the transformation from the orthorhombic to the monoclinic phase.

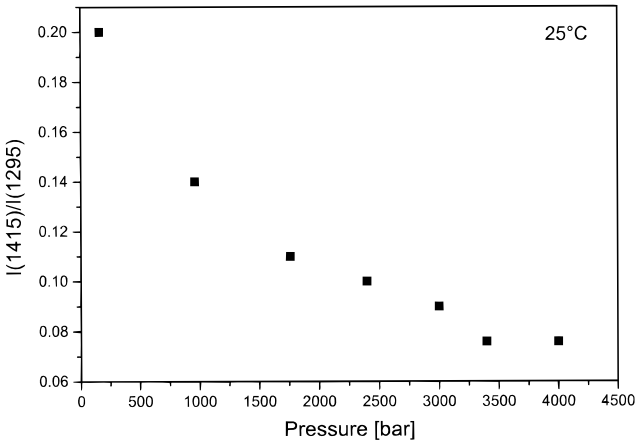

Figure 5. Ratio $I(1415)/I(1295)$ vs pressure for UHMW−PE at 25 °C. The decrease in the ratio is related to the disappearance of the orthorhombic phase.

crystal field splitting in the spectral range of the bending mode. Because of the complications in the 1415−1460 cm^{-1} spectral range due to Fermi resonance, which are discussed in detail in section 3, quantification of the changes within CH_2 bending region becomes difficult and is not free of ambiguity. Using the intensity ratio $(I_{1415}/(I_{1440} + I_{1470}))$[39] as a quantification measure of the phase transformations in polyethylene from the orthorhombic into the monoclinic phase, as suggested in section 3, is not completely appropriate. Namely, the changes in the ratio $(I_{1415}/(I_{1440} + I_{1470}))$ could be also assigned to the changes of the setting angle, which may occur within the orthorhombic lattice as an influence of pressure. To follow changes in the concentration of the orthorhombic modification within the sample we have alternatively used the intensity ratio of the 1415 and 1295 cm^{-1} bands because the latter is very much *in*dependent of chain conformation[33,34] and is therefore often used as an internal reference. The results are shown in Figure 5. When the pressure is raised, up to 4000 bar, the intensity ratio between 1415 and 1295 cm^{-1} bands decreases gradually from about 0.2 to 0.07. Disappearance of the band at 1415 cm^{-1} indicates that the concentration of the orthorhombic phase, characterized by two chains per unit cell, decreases while raising pressure. The X-ray results (Figure 3) suggest that upon raising pressure at room temperature the phase transformation from the orthorhombic to the monoclinic phase takes place. As the monoclinic phase gets dominant, the band at 1415 cm^{-1} loses intensity indicating the disappearance of the orthorhombic crystal structure within the sample. The disappearance of the crystal field splitting is related to the fact that the monoclinic unit cell possesses one molecular chain per unit cell. From lattice dynamics it is well established that for the monoclinic (and hexagonal) modification(s) the dynamics

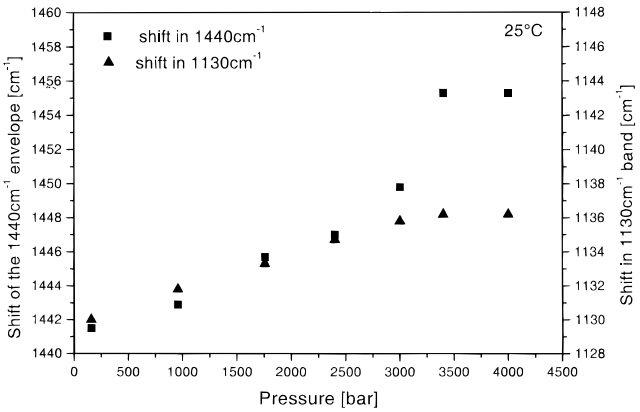

Figure 6. Frequency shift of the 1440 cm^{-1} envelope and 1130 cm^{-1} band as a function of applied pressure at room temperature.

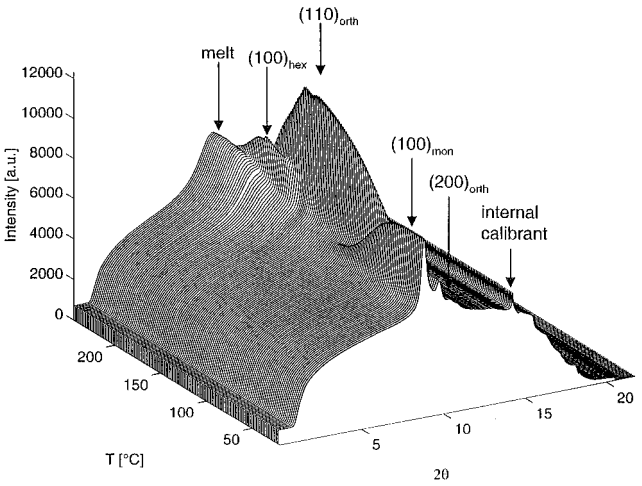

Figure 7. 3-D plot of WAXS integrated patterns recorded in situ on heating UHMW−PE at fixed pressure of 4000 bar. Initially strong (100) monoclinic and relatively weak (110) and (200) orthorhombic reflections can be observed. In the course of heating the (100) monoclinic reflection disappears while the (110) and (200) orthorhombic ones gain in the intensity. At about 120 °C the (100) monoclinic reflection completely disappears while the orthorhombic (110) and (200) reflections dominate the diffractogram. In the course of heating, about 215 °C, the (100) hexagonal phase appears and it strengthens on further heating. In the temperature range 225−230 °C, the hexagonal phase becomes dominant while the orthorhombic (110) and (200) reflections completely vanish. In this region amorphous halo appears and sample finally melts via the hexagonal phase. Internal calibrant shown in the figure results from the edges of the CCD detector dimensions.

of the single and isolated unit cell is a very acceptable approximation.[46,47] Dispersion curves of single chain polyethylene have been a matter of many studies. For the orthorhombic lattice each dispersion curve splits into a pair whose separation depends on the intermolecular forces; i.e., $k = 0$ modes are then split into doublets,[46,48] and their relative intensities are function of the setting angle.[38] Each doublet becomes a singlet for monoclinic and hexagonal lattices. Difference in $k = 0$ modes for the latter two structures may be only slightly different because of electrical field effects. Additionally, a pronounced shift in the frequency of the single line at 1440 cm^{-1} takes place with increasing pressure (Figure 6) as the crystal transforms from the orthorhombic to the monoclinic phase. The 1440 cm^{-1} envelope shifts to a maximum value of 1455 cm^{-1} at pressure of 3400 bar. Simultaneously, a small shift in the 1470 cm^{-1} band to higher frequency is also observed whereas the band at 1415 cm^{-1} does not change in frequency. In the region of the orth → mon transformation the band at 1060 cm^{-1} (asymmetric C−C stretching) stays unchanged while the band at 1130 cm^{-1} (symmetric C−C stretching) exhibits pronounced shift to the higher frequencies (as observed in Figure 6). These observations may appear to be in disagreement with the results obtained for long *n*-alkanes where the frequencies of the orthorhombic, monoclinic, or triclinic lattices (at room temperature and atmospheric pressure) do not shift as much as by polyethylene (at high pressure). An explanation for this discrepancy can be a consequence of shrinkage in the intermolecular distances with increasing pressure (as observe by X-ray in Figure 3). As a result of shrinkage intermolecular forces stiffen and frequencies of the modes which mostly probe the environment around the chain raise their frequencies. At the same time the intensities of the both skeletal vibrations (at 1060 and 1130 cm^{-1}) relative to the intensity of the internal standard (1295 cm^{-1}) stay unchanged (crystal field splitting can only be observed at low temperatures for these bands, and is only a few wavenumbers in magnitude). These results confirm that though the large part of crystals in the bulk no longer exists in the orthorhombic phase the chain conformation remains unaltered, in line with the X-ray observations. The weak band at 1415 cm^{-1} stays even at 4000 bar due to the fact that not all the crystals have transformed into the monoclinic phase as shown by WAXS data in Figure 3f.

4.2 Heating the Sample at 4000 bar. Figure 7 shows a 3-D plot of WAXS integrated patterns recorded in situ during heating at 4000 bar. In the course of heating the (100) monoclinic reflection diminishes while the orthorhombic (110) and (200) reflections intensify, indicating the transformation from monoclinic to orthorhombic crystal structure. This may be explained as a release in shear constraints on heating.[27] Upon further heating at 4000 bar, the (100) hexagonal reflection appears and gains in intensity while the orthorhombic (110) and (200) reflections diminish. In the temperature interval between 225 and 230 °C the hexagonal (100) reflection stays while the orthorhombic (110) and (200) reflections nearly vanish. This confirms the equilibrium stability region for the hexagonal phase at 4000 bar.[4,5] As the sample is heated further isobarically, the amorphous halo starts appearing and it intensifies while the hexagonal (100) reflection decreases in intensity indicating melting of the hexagonal crystals.

All the three phase transformations, mon → orth, orth → hex, and hex → melt, have been followed in situ by Raman spectroscopy as shown in Figures 8 and 11. Figure 8 shows the Raman spectra recorded in situ when heating the sample from 25 to 150 °C at 4000 bar. In this temperature region the mon → orth transformation takes place as observed by X-ray diffraction (Figure 7). The discussion will be again restricted to the relative changes occurring in the CH_2 bending (1400−1500 cm^{-1}) and C−C skeletal region (1000−1200 cm^{-1}) of the spectrum. Once more, the changes in the concentration of the orthorhombic crystal lattice within the sample will be performed by showing intensity ratio between the 1415 and 1295 cm^{-1} bands, as discussed in the previous section. If compared with WAXS data (Figure 7), it can be observed that the ratio $I(1415)/I(1295)$ increases precisely in the temperature region corresponding to the change in the unit cell from the

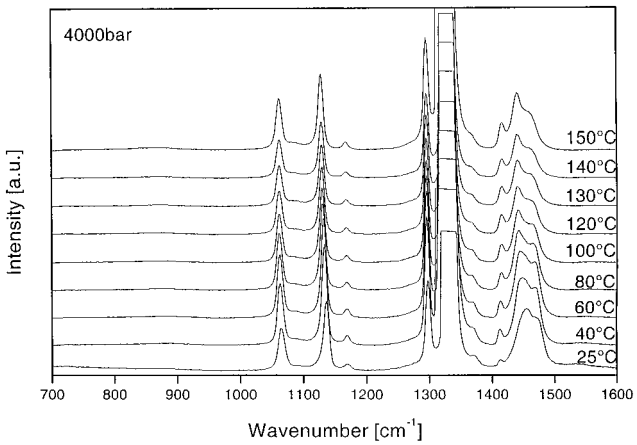

Figure 8. Raman spectra of UHMW−PE recorded in situ on raising temperature from 25 to 150 °C at a fixed pressure of 4000 bar. The figure comprises the temperature range of the monoclinic to orthorhombic transition.

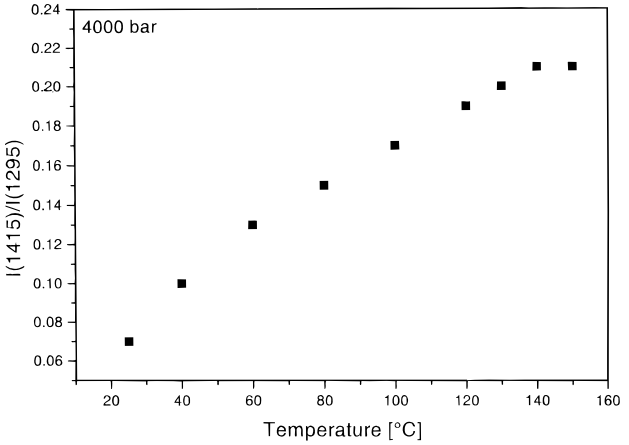

Figure 9. $I(1415)/I(1295)$ vs temperature plot for UHMW−PE at fixed pressure of 4000 bar. The increase in the ratio is related to the reappearance of the orthorhombic phase.

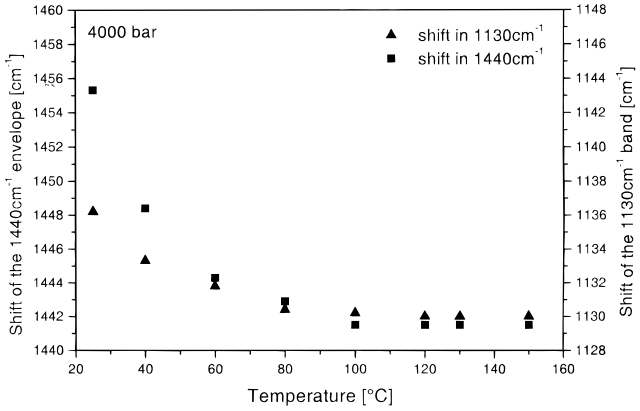

Figure 10. Frequency shift of the 1440 cm^{-1} envelope and 1130 cm^{-1} band as a function of temperature raised at pressure of 4000 bar.

monoclinic to the orthorhombic phase (Figure 9). Once all crystals have transformed back to the orthorhombic crystal structure, i.e., above 120 °C, the ratio $I(1415)/I(1295)$ stays constant. While temperature is being raised at 4000 bar, during the mon → orth transformation, the 1440 cm^{-1} envelope shifts back to the lower values of wavenumbers. Figure 10 shows that the single line shifts from 1455 cm^{-1} back to the value of 1440 cm^{-1}, which has been the starting point before raising

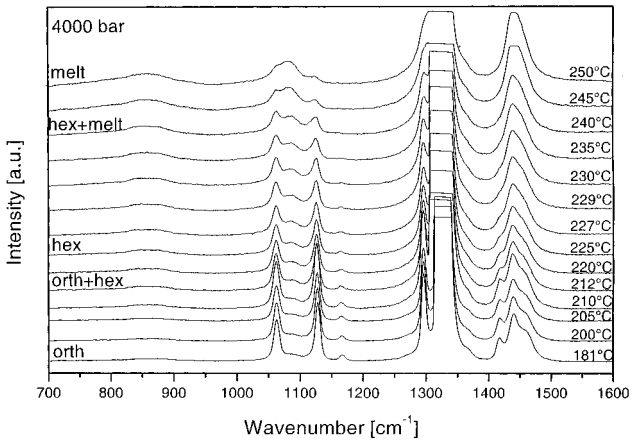

Figure 11. Raman spectra of UHMW−PE recorded in situ on raising temperature from 181 to 250 °C at a fixed pressure of 4000 bar. The figure comprises the temperature range of the orthorhombic to hexagonal and the hexagonal to melt transition.

the pressure at room temperature. The same trend has been observed in the skeletal mode of the spectrum. Once the transformation from the monoclinic to the orthorhombic phase takes place the symmetric C−C stretching band now positioned at around 1136 cm^{-1} shifts back to its initial position at 1130 cm^{-1} (Figure 10). Again no changes in the intensity ratio of the two skeletal vibrations at 1060 and 1130 cm^{-1} with respect to 1295 cm^{-1} band (internal standard) has been observed during the mon → orth transformation, which confirms that no change in the chain conformation takes place.

Figure 11 shows the Raman spectra of UHMW−PE on heating the sample, in the temperature region between 180 and 250 °C, i.e., the region comprising the orth → hex and the hex → melt transitions as shown by the WAXS integrated pattern in Figure 7. The starting spectrum in Figure 11 is typical for semicrystalline polyethylene with orthorhombic unit cell as discussed previously. Upon heating, the 1440 cm^{-1} band broadens while the 1415 cm^{-1} loses intensity. Since the 1000−1200 cm^{-1} spectral region is essentially unaffected within the region of the orthorhombic phase, the overall crystallinity level is constant and the features observed in the 1400−1500 cm^{-1} spectral region can be attributed to a change in crystal structure. In the region of mixed orthorhombic and hexagonal crystals (212−225 °C) the 1415 cm^{-1} band stays in the form of a shoulder attached to the band centered at 1440 cm^{-1}. When the region of the equilibrium stability of the hexagonal phase (between 225 and 230 °C) is entered, the triplet loses its form and only a broad single band centered at 1440 cm^{-1} can be observed within the bending region. In the spectrum of the hexagonal phase the frequency shifts of the 1440 and 1130 cm^{-1} bands with respect to their position in the orthorhombic phase are not observed. This is in contrast with the results obtained for the monoclinic phase where the frequency shift of the 1440 as well as the 1130 cm^{-1} band to the higher values of wavenumbers has been shown. In the region of the orth → hex transformation, the band at 1080 cm^{-1} starts appearing, suggesting the initiation of gauche defects in the regular trans zigzag conformation. An additional broad band around 870 cm^{-1} can be observed in the spectrum of the pure hexagonal phase (temperature region between 235 and 240 °C). The

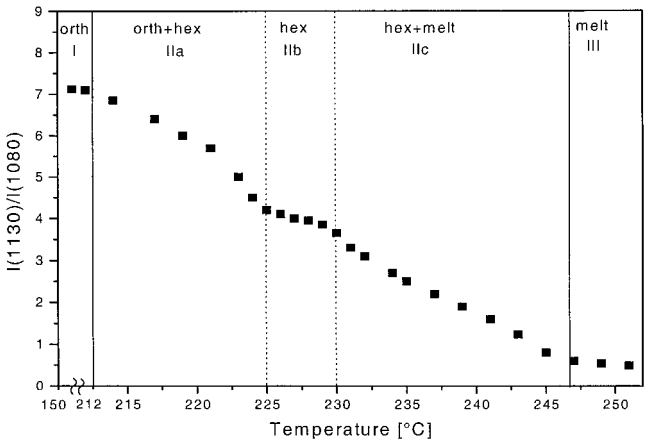

Figure 12. *I*(1130)/*I*(1080) vs temperature plot for UHMW−PE at fixed pressure of 4000 bar. The temperature range is divided into three temperature regions according to the X-ray results. Region I is the region of the pure orthorhombic phase. In region II, the intervention of the hexagonal phase becomes prominent. The region is subdivided into three separate subregions: the orthorhombic to hexagonal transition region (IIa), the pure hexagonal phase (IIb), and the melting region of the hexagonal phase (IIc). Region III is the region of the pure melt.

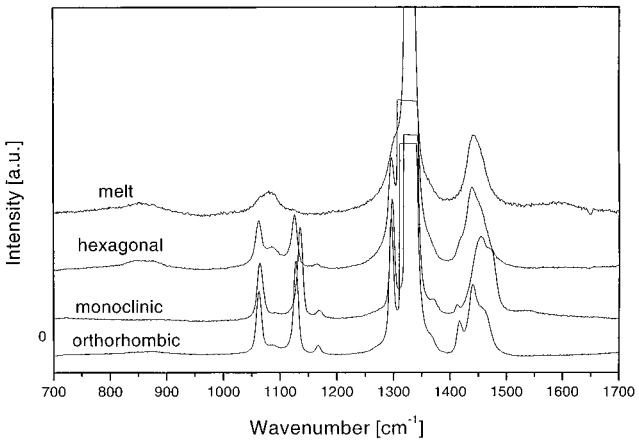

Figure 13. Composite figure showing Raman spectra of the orthorhombic phase, the monoclinic phase, the hexagonal phase, and the melt.

existence of this band in the spectrum of polyethylene melt has been reported before and is considered to be the additional feature of the gauche content within the chain.[35,43,49] Though present, the intensity of the amorphous band at 1080 cm^{-1} stays relatively weak throughout the narrow region of the hexagonal phase leaving the bands at 1060 and 1130 cm^{-1} dominant in the skeletal region of the spectrum. As the amorphous content starts increasing (appearance of the amorphous halo in Figure 7) indicating melting of hexagonal crystals, the band at 1080 cm^{-1} intensifies while the bands at 1060 and 1130 cm^{-1} start disappearing. The changes in the chain conformation (i.e., trans content) during the orth → hex and hex → melt transition are given in Figure 12 and are expressed as the intensity ratio of the skeletal 1130 cm^{-1} and the gauche 1080 cm^{-1} bands vs temperature. The figure is divided into three separate regions, the vertical lines being drawn from the experimental observations made by in situ X-ray studies. The region I (from 120 to 212 °C) is a temperature region of the orthorhombic phase. Here, the intensity ratio between 1130 and 1080 cm^{-1} is high and does not change while increasing pressure or temperature. The temperature region comprising the hexagonal phase is divided into three subregions, IIa, IIb, and IIc. In subregion IIa, the orth → hex transition starts at about 212 °C and can be distinguished in Figure 12 by the subsequent decrease of the characteristic intensity ratio. In subregion IIb, the stability region of the hexagonal phase at pressure of 4000 bar (between 225 and 230 °C), a clear decrease in the slope *I*(1130)/*I*(1080) vs *T* can be observed. Upon raising the temperature further the amorphous halo intervenes (as discussed in Figure 7) and the gauche content slowly increases (i.e., *I*(1130)/*I*(1080) decreases) due to the partial melting of hexagonal crystals (region IIc). Once the sample is melted, the characteristic intensity ratio stays constant giving a value typical for the melt (region III). The decrease in the trans content, within region II, is not continuous (intervention of region IIb, Figure 12), and that implies that a clear distinction between the hexagonal phase and the melt can be obtained by Raman spectroscopy.

Figure 13 is a composite picture of the Raman spectra of the orthorhombic phase, the monoclinic phase, the hexagonal phase, and the melt. From here it is evident that the Raman spectrum of the hexagonal phase is similar to that of the rotor phase in paraffins.[49] Though our results are dissimilar from earlier observations made by Tashiro et al.,[23] the difference may be due to different experimental conditions. The drop in the intensity ratio *I*(1130)/*I*(1080) from 7.8 (region I; Figure 12) to 4 (region IIb, Figure 12) suggests a relative increase in the gauche content in the hexagonal phase at 4000 bar. Sufficiently high trans content within the hexagonal phase compared to that of the melt results in feasible distinction between the hexagonal phase and the melt. To strengthen our observations, in situ Raman results on melting the same UHMW−PE at atmospheric pressure, i.e., without the intervention of the hexagonal phase, are shown in Figure 14. Here the continuous increase in the intensity of the gauche band at 1080 cm^{-1} can be seen above 115 °C, on raising temperature. As the gauche band increases in the intensity, the crystal field splitting (1415/1440 cm^{-1}) in the bending mode disappears continuously and around 143 °C only a broad band centered around 1440 cm^{-1} can be observed within the bending region. Within the skeletal region of the Raman spectrum at 143 °C only the gauche band at 1080 cm^{-1} can be seen. The continuous change of gauche content when melting the UHMW−PE powder via orthorhombic phase is shown in Figure 14b where the ratio *I*(1130)/*I*(1080) vs *T* is plotted the same way as in the Figure 12. Upon melting of UHMW−PE powder at atmospheric pressure, the characteristic ratio *I*(1130)/(1080) (measure of the trans content) decreases continuously within the temperature range of about 20 °C, not revealing any disturbance like the plateau in the Figure 12 (region IIb). This was confirmed by DSC measurements performed on the same UHMW−PE powder under the same conditions as the Raman experiments at atmospheric conditions where melting point at 143 °C and the width of the melting peak of about 20 °C could be observed. In the case of melting UHMW−PE at 4000bar, the temperature range of the melting becomes wider (∼32 °C) showing clearly two different conformational regions due to the intervention of the, intermediate hexagonal phase.

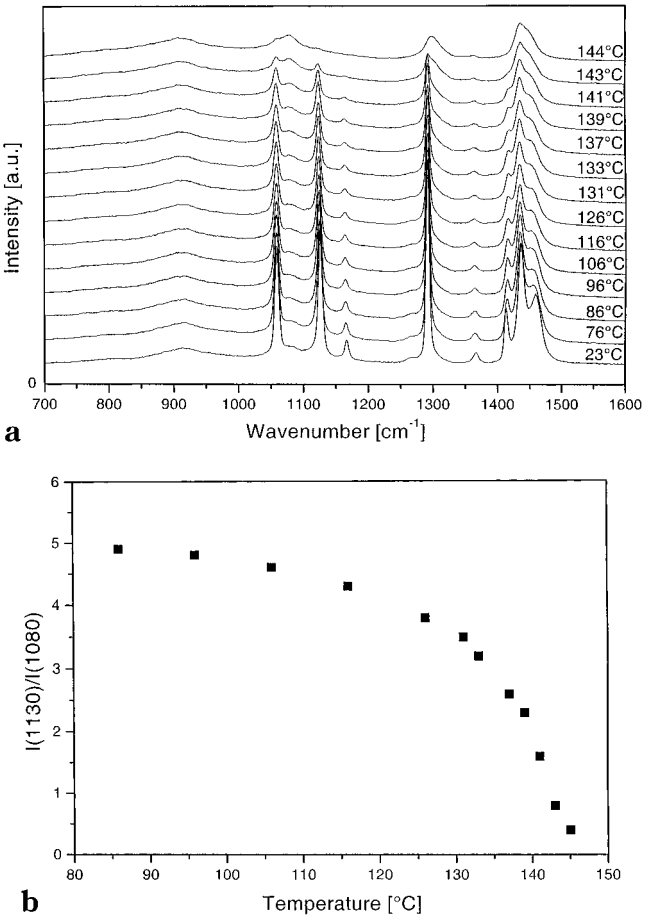

Figure 14. Results on in situ Raman spectroscopy of UHMW−PE powder at ambient conditions using Linkam hotstage: (a) Raman spectra recorded in situ when heating UHMW−PE powder to 150 °C with a rate of 2 °C/min: (b) $I(1130)/I(1080)$ vs temperature plot for UHMW−PE at ambient pressure.

Observations similar to that at atmospheric pressure were also observed by Raman spectroscopy when a sample of UHMW−PE having thick crystals (>50 nm) was melted at the pressures below 3.6kbar. It is to be noted that WAXS studies suggest that the sample having thick crystals, directly melts from the orthorhombic phase on heating below 3.6 kbar.[12]

5. Conclusions

The first observations of the phase transformations in polyethylene under elevated pressure using in situ X-ray and Raman spectroscopy under the same experimental conditions have been presented in this paper. X-ray analysis has been used to explore the phase diagram of polyethylene. From the work presented in this paper it is shown conclusively that the combination of X-ray with Raman spectroscopy can provide information on structural and conformational changes during phase transformations.

To distinguish between different phases in polyethylene the bending mode of the Raman spectrum was discussed in combination with the skeletal one (1000−1200 cm^{-1}), providing a measure for the conformational changes.

Our experimental observations suggest that a clear distinction can be made between the orthorhombic, hexagonal/monoclinic phase within the bending region of the spectrum, most clearly shown by the spectra displayed in Figure 13. The orthorhombic phase is characterized by the well resolved triplet within the bending region of the spectrum. The characteristic form of the bending mode results from the crystal field splitting which is a consequence of the presence of two chains within the orthorhombic unit cell. On the other hand, the monoclinic and the hexagonal phase, having one chain per unit cell, do not exhibit the 1415 cm^{-1} band (or it is greatly reduced attributed to coexistence of phases) but the single line at about 1440 cm^{-1}. The 1440 cm^{-1} band shifts to higher frequencies with increase in pressure. The pronounced shift in the 1130 cm^{-1} band within the skeletal region of the spectrum has also been observed for the monoclinic phase whereas its position stays the same for the orthorhombic and the hexagonal phase. The intensity of the skeletal bands within the 1000−1200 cm^{-1} spectral range does not change for the orthorhombic and monoclinic phase (low-temperature experiments would have revealed crystal field splitting also here), whereas for the hexagonal phase a significant increase in the intensity of the gauche band at 1080 cm^{-1} can be observed.

From the results presented in this paper it becomes obvious that the phase transformations in polyethylene can be followed quantitatively in the skeletal range of the spectrum. Because of the complications within the bending mode, which are discussed in details within the paper, it has been shown that the phase changes in polyethylene can be followed qualitatively (due to the presence of the crystal field splitting) but the quantification of the changes becomes ambiguous.

Acknowledgment. The authors would like to acknowledge the X-ray facilities available on beamline ID11/BL2 at the European Synchrotron Radiation Facilities, Grenoble, France.

References and Notes

(1) Wunderlich, B. *Macromolecular physics*; Academic Press: New York 1976; Vol. 2.
(2) Keller, A.; Hikosaka, M.; Rastogi, S.; Toda, A.; Barham, P. J.; Gooldbeck-Wood, G. *J. Mater. Sci.* **1994**, *29*, 2579; *Philos. Trans. R. Soc. London* **1994**, *A348*, 3.
(3) Keller, A. *Philos. Mag.* **1957**, *2*, 1171.
(4) Basset, D. C.; Khaifa, A.; Turner, B. *Nature (London)* **1972**, *106*, 239; **1972**, *240*, 146.
(5) Basset, D. C. *Polymer* **1976**, *17*, 460.
(6) Rastogi, S.; Hikosaka, M.; Kawabata, H. J.; Keller, A. *Macromolecules* **1991**, *24*, 9384.
(7) Wunderlich, B.; Grebovicz, J. *Adv. Polym. Sci.* **1984**, *60/61*, 1.
(8) Hikosaka, M. *Polymer* **1987**, *28*, 1257; **1990**, *31*, 458.
(9) Basset, D. C.; Block, S.; Piermarini, G. J. *J. Appl. Phys.* **1974**, *45*, 4146.
(10) Basset, D. C. *The crystallisation of polyethylene at high pressures in Developments in crystalline polymers*; Basset, D. C., Ed.; Applied Science: London, 1982; pp 115−151.
(11) Hikosaka, M.; Rastogi, S.; Keller, A.; Kawabata, H. J. *Macromol. Sci.-Phys* **1992**, *B31* (1), 87.
(12) Rastogi, S.; Kurelec, L.; Lemstra, P. J. *Macromolecules* **1998**, *31*, 5022.
(13) Basset, D. C.; Turner, B. *Philos. Mag.* **1974**, *29*, 925.
(14) Yasuniwa, M.; Takemura, T. *Polymer* **1974**, *15*, 661.
(15) Maeda, Y.; Kanetsuna; H. *J. Polym. Sci., Polym. Phys. Ed.* **1974**, *12*, 2551.
(16) Maeda, Y.; Kanetsuna, H. *J. Polym. Sci., Polym. Phys. Ed.* **1975**, *13*, 637; **1976**, *14*, 2057.
(17) Yasuniwa, M.; Enoshita, R.; Takemura, T. *Jpn. J. Appl. Phys.* **1976**, *15*, 1421.
(18) Yamamoto, T.; Miyaji, H.; Asai, K. *Jpn. J. Appl. Phys.* **1977**, *16*, 1891.
(19) Takemura, T. *Polym. Prepr.* **1979**, *20*, 270.
(20) de Langen, M. Ph.D. Thesis, University Amsterdam, 1998.
(21) Tanaka, T.; Takemura, T. *Polym. J.* **1980**, *12*, 355.
(22) Wunder, S. L. *Macromolecules* **1981**, *14*, 1024.

(23) Tashiro, K.; Sasaki, S.; Kobayashi, M. *Macromolecules* **1996**, *29*, 7460.
(24) Pennings, A. J.; Zwijnenburg, A. *J. Polym. Sci., Polym. Phys. Ed.* **1979**, *17*, 1011.
(25) Lemstra, P. J.; van Aerle, N. A. J. M.; Bastiaansen, C. W. M. *Polym. J.* **1987**, *19*, 85.
(26) Cho, Y.; Kobayashi, M.; Tadokoro, H. *Polym. Prepr. Jpn.* **1986**, *30*, 1842.
(27) Seto, T.; Hara, T.; Tanaka, K. *Jpn. J. Appl. Phys.* **1968**, *1*, 31.
(28) Allan, P.; Bevis, M. *Philos. Mag.* **1975**, *31*, 1001 **1977**, *35*, 405.
(29) Young, R. J.; Bowden, P. B. *Philos. Mag.* **1974**, *29*, 1061.
(30) Bevis, M.; Crellin, E. B. *Polymer* **1971**, *12*, 666.
(31) Hikosaka, M.; Seto, T. *Jpn. J. Appl. Phys.* **1982**, *21*, L332.
(32) Amstrong, B. H. *J. Quantum Spectrosc. Radioat. Transfer* **1967**, *7*, 61.
(33) Gall, M. J.; Hendra, P. J.; Peacock, C. J.; Cudby, M. E.; Willis, H. A. *Spectrochim. Acta* **1972**, *28A*, 1485.
(34) Strobl, G. R.; Hagedorn, W. *J. Polym. Sci., Polym. Phys. Ed.* **1978**, *16*, 1181.
(35) Koglin, E.; Meier, R. J. *Comput. Theor. Polym. Sci.* **1999**, *9*, 327.
(36) Bower, D. I.; Maddams, W. F. *The vibrational spectroscopy of polymers*; Cambridge University Press: Cambridge, England, 1989.
(37) Masetti, G.; Abbate, S.; Gussoni, M.; Zerbi, G. *J. Chem. Phys.* **1980**, *73*, 4671.
(38) Abbate, S.; Gussoni, M.; Zerbi, G. *J. Chem. Phys.* **1980**, *73*, 4680.
(39) Abbate, S.; Zerbi, G.; Wunder, S. L. *J. Chem. Phys.* **1982**, *86*, 3140.
(40) Boerio, F. J.; Koenig, J. L. *J. Chem. Phys.* **1970**, *52*, 3425.
(41) Snyder, R. G.; Hsu, S. L.; Krimm, S. *Spectrochim. Acta* **1978**, *34A*, 395.
(42) Barnes, J. D.; Fanconi, B. M. *J. Chem. Phys.* **1972**, *56*, 5190.
(43) Kim, Y.; Strauss, H. L.; Snyder, R. G. *J. Phys. Chem.* **1989**, *93*, 7520.
(44) Ungar, G. *Macromolecules* **1986**, *19*, 1317.
(45) Ottani, S.; Porter, R. S. *Polymer* **1990**, *31*, 369.
(46) Tasumi, M.; Krimm, S. *J. Chem. Phys.* **1967**, *46*, 755.
(47) Tasumi, M.; Shimanouchi, T. *J. Chem. Phys.* **1965**, *43*, 1245.
(48) Snyder, R. G. *J. Chem. Phys.* **1979**, *71*, 3229.
(49) Mutter, R.; Stille, W.; Strobl, G. *J. Polym. Phys* **1993**, *31*, 99.

MA9911187